Revista Mexicana de Biodiversidad

Revista Mexicana de Biodiversidad 97 (2026): e975764

Taxonomy and systematics

Redescription of *Stagmomantis hebardi* (Mantodea: Mantidae), with the description of the female

Redescripción de Stagmomantis hebardi *(Mantodea: Mantidae), con la descripción de la hembra*

Aarón Emilio Vásquez-Quintero [a], Iker Cubillos-Macías [b], Erick Omar Martínez-Luque [c], Jovana M. Jasso-Martínez [b], Fernando Varela-Hernández [a, *]

[a] *Universidad Autónoma del Estado de Morelos, Escuela de Estudios Superiores del Jicarero, Laboratorio de Sistemática Molecular, Carretera Galeana-Tequesquitengo s/n, Col. El Jicarero, 62909 Jojutla, Morelos, Mexico*

[b] *Universidad Nacional Autónoma de México, Instituto de Biología, Colección Nacional de Insectos, Tercer Circuito Exterior s/n, Cd. Universitaria, Copilco El Alto, Coyoacán, Apartado postal 70-233, 04510 Mexico City, Mexico*

[c] *Universidad Autónoma de Querétaro, Facultad de Ciencias Naturales, Av. de las Ciencias s/n, Juriquilla, 76230 Querétaro, Querétaro, Mexico*

*Corresponding author: fernando.varela@uaem.mx (F. Varela-Hernández)

Received: 02 September 2025; accepted: 08 December 2025

Abstract

The genus *Stagmomantis* Saussure, 1869 comprises a group of New World mantids whose taxonomic delimitation and composition have been challenging due to complex morphological variation. *Stagmomantis hebardi* Rehn, 1935, a species distributed in the Neotropical region and the Mexican Transition Zone, was originally described based on both a female and a male specimen. However, the female was subsequently recognized as belonging to a different species within the subgenus *Auromantis*. In this study, we provide the redescription of the male and the description of the female of *S. hebardi*. Descriptions are based on external morphology and both sexes internal genitalia characters. The conspecificity of the male and female is supported by molecular evidence provided in previous studies and further validated by biological observations from captive rearing. The corkscrew-like pda (posterior process of the ventral phallomere) in the male genitalia and the lobe-like structure between the fifth and sixth tergites in the female abdomen are diagnostic characters that distinguish this species from others of the genus *Stagmomantis*.

Keywords: External morphology; Internal genitalia; Mantids; Taxonomic description

ISSN versión electrónica: 2007-8706; Universidad Nacional Autónoma de México, Instituto de Biología. https://doi.org/10.22201/20078706e.2026.97.5764

Resumen

El género *Stagmomantis* Saussure, 1869 es un grupo de mantis del Nuevo Mundo cuya delimitación y composición han sido desafiantes debido a su compleja variación morfológica. *Stagmomantis hebardi* Rehn, 1935, una especie distribuida en la región Neotropical y la Zona de Transición Mexicana, fue descrita originalmente con base en un macho y una hembra. Más tarde, se reconoció que la hembra pertenecía a una especie diferente del subgénero *Auromantis*. En este estudio, proporcionamos la redescripción del macho y la descripción de la hembra de *S. hebardi*. Ambas descripciones se basan en caracteres de morfología externa y de la genitalia de ambos sexos. La asociación específica entre el macho y la hembra está respaldada por análisis moleculares previos y validada por observación directa en cautiverio. El pda (proceso posterior del falómero ventral) en forma de sacacorchos en la genitalia del macho y la estructura en forma de lóbulo entre los terguitos quinto y sexto en el abdomen de la hembra son caracteres clave para separar a esta especie de otras del género *Stagmomantis*.

Palabras clave: Morfología externa; Genitalia interna; Mantis; Descripción taxonómica

Introduction

The order Mantodea (praying mantises) comprises about 2,500 species worldwide, distributed in 16 superfamilies, 29 families, 60 subfamilies, and 436 genera (Ehrmann, 2002; Otte & Spearman, 2005; Schwarz & Roy, 2019). Mantidae Latreille, 1802 is the most species-rich family, containing approximately half of the described species (Patel & Singh, 2016; Svenson & Whiting, 2004, 2009); however, the limits and phylogenetic relationships within Mantidae remain unclear. Several groups previously defined based on morphological data were later recovered as non-monophyletic by analyses using mitochondrial and nuclear genes (Svenson & Whiting, 2004, 2009), as well as mitochondrial genomes (Wang et al., 2022; Xu et al., 2021).

Stagmomantis Saussure, 1869 is a New World genus belonging to the subfamily Stagmomantinae Giglio-Tos, 1919. It is one of the most species-rich genera within Mantidae, with 25 recognized species (Anderson, 2025). Species delimitation within *Stagmomantis* has been challenging due to significant morphological variation among its members, rendering the number of valid species debatable (Agudelo-Rondón et al., 2007; Anderson, 2020a, b, 2021; Ehrmann, 2002; Maxwell, 2014; Otte & Spearman, 2005; Terra, 1995). For instance, Maxwell (2014) did not recognize *S. conspurcata* Serville, 1869 as a valid species, treating it as a synonym of *S. carolina* (Johansson, 1763). Later, Anderson (2020b) revalidated *S. conspurcata*, arguing that sufficient morphological differences —such as body size and male hindwing coloration— justified its recognition as a distinct species. This case exemplifies the taxonomic instability present within *Stagmomantis*, which has important implications, such as constant changes in the reported geographic distribution patterns of its species.

In 1935, Rehn described *Stagmomantis hebardi* —named after the American entomologist Morgan Hebard— based on a female and a male specimen from Sinaloa, Mexico. Hebard (1923) had previously identified these specimens as *S. limbata* Hahn, 1835 and *S. tolteca* Saussure, 1861, respectively. In his description, Rehn included images of the dorsal habitus of both the female and male, as well as an illustration of the male's internal genitalia. The taxonomic status of *S. hebardi*, based on the male-female association established by Rehn, has remained unchallenged for decades.

Recently, a molecular analysis grouped together a female and a male specimen previously identified as *S. carolina* (Varela-Hernández et al., 2022). In addition to the molecular data, that study included high-resolution images of the dorsal habitus. Subsequent comparison of those specimens with the descriptions and illustrations in Rehn (1935) revealed that the male assigned to *S. carolina* corresponded to *S. hebardi*. Crucially, the morphological traits of the female described as *S. hebardi* by Rehn (1935) did not match those of the female specimen molecularly associated with the male in Varela-Hernández et al. (2022).

Based on this evidence, we consider that Rehn (1935) erroneously associated the sexes of *S. hebardi*, establishing a heterospecific type series. Consequently, the main objectives of this study are to correctly associate both sexes of *S. hebardi*, to redescribe the male, and to formally describe the female of *S. hebardi* (Rehn, 1935). This work is supported by the aforementioned molecular evidence and is based on external morphology as well as a comprehensive analysis of male and female genitalia.

Materials and methods

A total of 48 pinned specimens identified as *Stagmomantis hebardi* were examined (29 males and 15

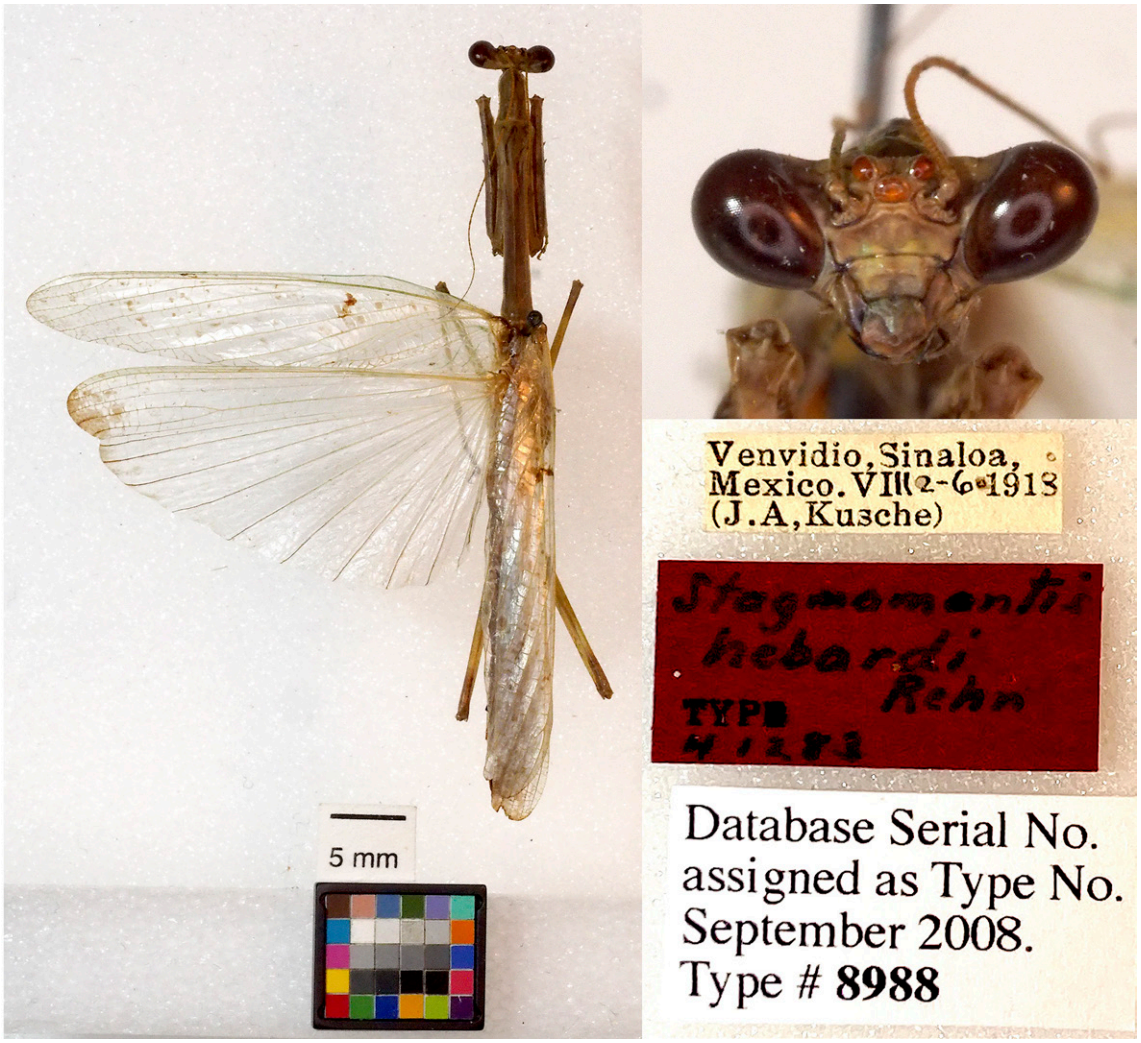

Figure 1. Holotype of *Stagmomantis hebardi* Rehn, 1935, Academy of Natural Sciences of Philadelphia (ANSP). Images provided by Jason D. Weintraub (ANSP Collection Manager).

females, see "Taxonomic summary"). These specimens are deposited at the Colección Nacional de Insectos, Instituto de Biología, Universidad Nacional Autónoma de México (CNIN-IBUNAM) and the Colección Entomológica de la Universidad Autónoma del Estado de Morelos, México (CEUAEM-MAN). Additionally, we examined high-resolution images of the holotype (Fig. 1) and allotype (Fig. 2) deposited at the Academy of Natural Sciences of Philadelphia (ANSP), USA.

Observations and measurements were conducted using an Olympus SZ stereomicroscope. Specimens identification at genus and species level followed the keys and descriptions provided by Rehn (1935), Agudelo-Rondón and Chica (2002), Maxwell (2014), and Anderson (2021). Specimens of both sexes were photographed from multiple angles using a Canon EOS Rebel T5 digital camera equipped with an EF 100 mm f/2.8 Macro USM lens. Camera control was managed via EOS Utility software; images were subsequently stacked and edited using Zerene Stacker and Photoshop CC 2019.

Terminalia of both sexes were softened in hot water (80-100 °C) for 15-20 min, following the protocol of Ferraz et al. (2023). Genitalia were then cleared in a 10% KOH solution at 40 °C for 20-30 min (Brannoch et al., 2017). The extraction of female genitalia followed the method described by Rodrigues and Cancello (2016). Cleared genitalia were rinsed twice in distilled water and stored in 70% ethanol. Remaining soft tissue was removed, and

Figure 2. Allotype of *Stagmomantis hebardi* Rehn, 1935, Academy of Natural Sciences of Philadelphia (ANSP). Images provided by Jason D. Weintraub (ANSP Collection Manager).

structures were photographed suspended in antibacterial gel to maintain their position (Su, 2016). Abbreviations for all measurements and genitalic structures are provided in Table 1.

To visualize the geographical distribution of the examined specimens, a map was generated using ArcGIS software, utilizing the State Geostatistical Framework, scale 1:250,000 (INEGI, 2024).

Description

Stagmomantis hebardi Rehn, 1935

Diagnosis. Male: distinguished by the corkscrew-like posterior process of the ventral phallomere (pda) (Fig. 3). Female: prosternum (inter-coxal area) blackish; anterior coxae armed with 3-6 blackish spines; presence of a protrusible lobe-like structure located between abdominal tergites 5 and 6 (Fig. 4).

Table 1

Abbreviations of male and female genitalia characters. Morphological characters follow Garikipati (2024) and genitalia characters follow Brannoch et al. (2017).

Morphological characters		Male genitalia characters		Female genitalia characters	
ACL:	Anterior coxae length	aafa:	Anterior lobe of phalloid apophysis (left phallomere)	agsl:	Accessory gland supporting lobe
AFL:	Anterior femur length				
AFW:	Anterior femur width	an:	Anterior extension of sclerite R3 (right phallomere)	CG8:	Caudogyne
ATL:	Anterior tibia length	bm:	Dextral extension (right phallomere)	CX8:	Coxa 8
AvS:	Anteroventral spines	fda:	Main posterior lobe (right phallomere)	cxdl:	Dorsolateral coxal lobelet
DS:	Discoidal spines	L4A:	Sclerite extending over the ventral wall (ventral phallomere)	cxvl:	Ventrolateral coxal lobelet
FwL:	Forewing length				
HH:	Head height	L4B:	Sclerite extending over the dorsal wall (left phallomere)	gl9:	Gonoplac 9
HW:	Head width				
HwL:	Hindwing length	loa:	Posteromesal (left phallomere)	gp8:	Gonapophysis 8
ML:	Metazone length	paa:	Posterior process (left phallomere)	gp9:	Gonapophysis 9
MFL:	Metafemur length	pafa:	Posterior lobe of phalloid apophysis (left phallomere)	gpal8:	Apical lobe of gonapophysis 8
MTL:	Metatibia length			gpmo8:	Medial outgrowth of gonapophysis 8
MsFL:	Mesofemur length	pda:	Posterior process (ventral phallomere)		
MsTL:	Mesotibia length	pia:	Process posterolateral to pva (right phallomere)	gptm9:	Medial tine of gonapophysis 9
PL:	Pronotum length				
PrL:	Prozone length	pva:	Process anteromesal to pia (right phallomere)	rh:	Rhachis
PvS:	Posteroventral spines			spb:	Spermathecal bulge
PW:	Pronotum width	R3:	Anteriorly extending sclerite (right phallomere)	vf7:	Ventral segmental fold 7
TL:	Total length	ssp:	Secondary spine	VS7:	Vestibular sclerite 7

Identification. Males: antennae longer than pronotum. Tubercle present between antennifer and compound eyes. Wings longer than abdomen; fore- and hindwings hyaline; costal area of forewings opaque with brown spots. Genitalia with the posterior process of ventral phallomere (pda) corkscrew-shaped. Females: abdominal tergites 4-6 dorsoventrally flattened; protrusible lobe-like structure present between tergites 5 and 6. Supragenital plate wider than long with well-developed longitudinal medial keel. Forewings opaque, greenish or brownish, with brown spots; hindwings opaque, anteriorly yellowish with brown spots near posterior margin, or yellowish with colorless spots posteriorly. Both sexes: ocellar tubercles absent; ocelli flush with surface of frons. Lower frons smooth, wider than long. Pronotum long and slender; lateral margins denticulate; dorsal surface smooth. Forecoxae approximately 3/4 the length of pronotum; anterior and posterior margins denticulate; forecoxal lobes convergent. Hearing organ of DK type.

Male (Fig. 5). Measurements (Table 2). Head: head capsule (Fig. 6a) with oval eyes; juxtaocular bulges undeveloped; ocellar tubercles undeveloped. Anterior margin of vertex straight, depressed near parietal sulcus. Ocelli larger than in females. A small tubercle present between antennifer and compound eye. Antennae filiform, longer than pronotum, reaching anterior portion of the

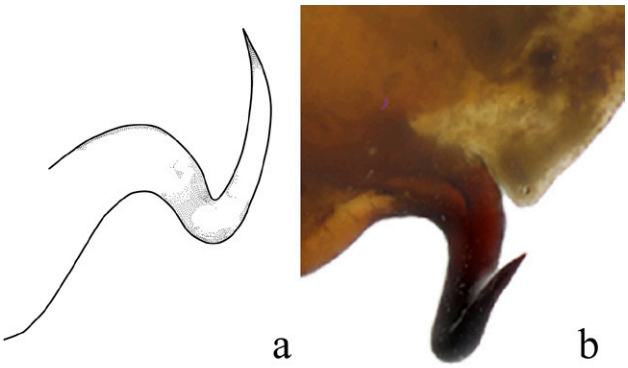

Figure 3. Comparison of the posterior process of ventral phallomere (pda) of the male genitalia of *Stagmomantis hebardi*. a) Illustration modified from Rehn (1935); b) specimen examined in this study.

mesothorax; pedicel nearly as long as scape. Frons wider than long, with an M-shaped depression in the middle of the transverse carina. Thorax: pronotum, supracoxal dilation slightly pronounced; supracoxal groove well-marked. Lateral margins of prozone denticulate; lateral margins of metazone denticulate, denticles decreasing in size posteriorly. In ventral view, inter-coxal area dark-colored. Legs: forelegs, spination formula: F = 4DS/12-15AvS/4PvS; T = 9-14AvS/9-11PsV. Forecoxae armed with 3-5 blunt, often blackish spines, small denticles interspersed between them; coxal lobes convergent (Fig. 6b). Forefemur relatively long, slender; femoral brush located at the level of last 3 posteroventral spines; tibial spur groove located at approximately the middle of femur; first discoidal spine smaller than the others; third discoidal spine longer than the others; blackish spot present at the level of first anteroventral spine (AvS). Foretarsus: distal portion of each segment darkened (Fig. 6c, d). Wings: slightly surpassing tip of abdomen. Forewings: hyaline, with scattered brown spots in discoidal area; stigma covered by dark brown patch; anterior margin wide at base, narrowing posteriorly; apex rounded. Hindwings: hyaline with a dark patch at apex; main central longitudinal veins feature a series of spotted brownish lines running along posterior margin to about half the distance to anterior margin (Fig. 5). Abdomen: slender, cylindrical. Subgenital plate longer than wide. Supragenital plate wider than long; apex rounded, with marked longitudinal medial keel. Cerci elongate; cercomeres cylindrical,

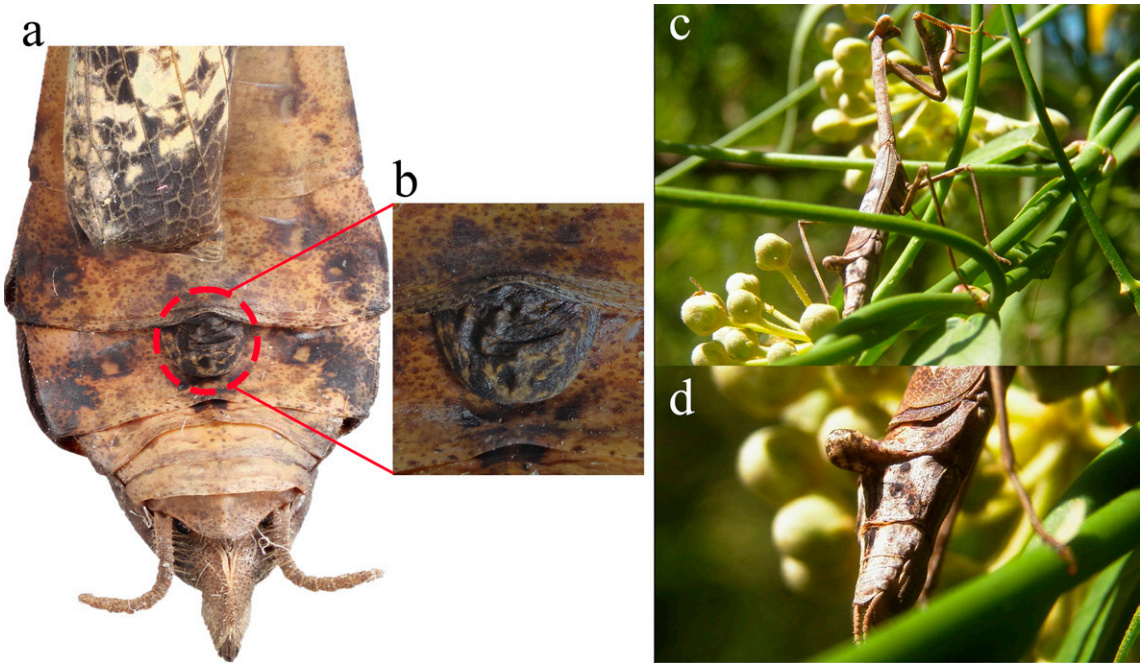

Figure 4. Protrusible lobe-like structure on the abdomen of female *Stagmomantis hebardi*. a-b) Dried specimen: a) dorsal view of the abdomen; b) close-up of the lobe-like structure (indicated in red). c-d) Live specimen: c) dorso-lateral view; d) close-up of the lobe-like structure. Specimens imaged: a-b (CEUAEM-MAN-139); c-d (iNaturalist observation 237796237, photo ID 423231786; photo by Edgar Salmerón Barrera).

Figure 5. Male of *Stagmomantis hebardi* (green/brown morphotype). a) Dorsal view; b) ventral view. Specimen imaged: CEUAEM-MAN-140. Scale bars = 10 mm.

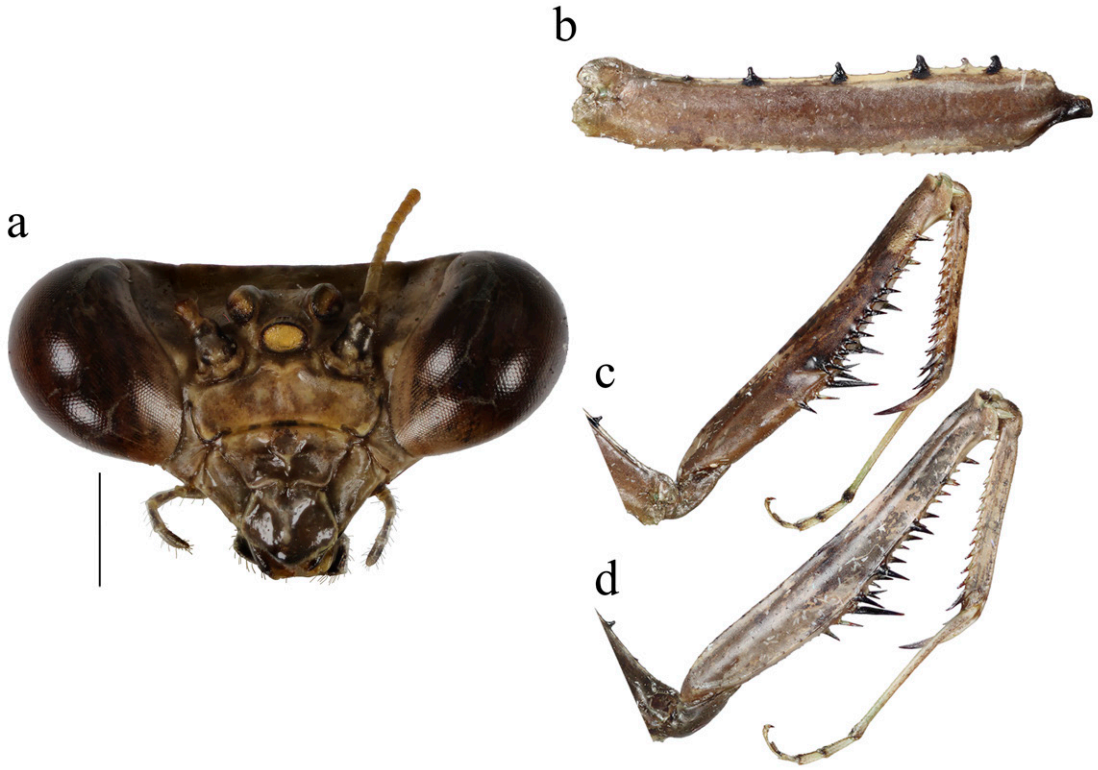

Figure 6. Morphological details of the male of *Stagmomantis hebardi*. a) Head capsule in frontal view; b) forecoxae in ventral view; c) forefemur and foretibia in ventral view; d) forefemur and foretibia in dorsal view. Specimens imaged: a (CEUAEM-MAN-021); b-d (CEUAEM-MAN-013). Scale bar = 1 mm (a); not to scale (b-d).

Table 2
Measurements (in mm) of males of *Stagmomantis hebardi* (*n* = 9).

Spec. ID	TL	PL	PrL	ML	PW	HH	HW	ACL	AFL
CEUAEM-MAN-140	51.0	16.5	3.5	13.0	2.5	4.0	5.0	8.5	9.5
CEUAEM-MAN-135	51.0	15.5	3.0	14.0	3.0	4.0	5.0	7.5	10.0
CEUAEM-MAN-013	55.0	18.0	4.0	14.5	3.0	4.0	5.5	9.0	11.0
CEUAEM-MAN-021	45.5	15.5	3.0	12.0	2.5	3.5	5.0	7.5	9.5
CEUAEM-MAN-015	47.0	16.5	4.0	12.5	2.5	4.0	5.0	8.0	10.0
CEUAEM-MAN-014	45.0	18.0	3.5	13.5	3.0	3.5	5.5	8.5	10.5
IBUNAM: CNIN: MA645	64.0	21.5	3.5	18.0	3.5	–	–	–	12.0
IBUNAM: CNIN: MA810	55.5	19.0	3.0	16.0	3.0	–	–	–	11.0
IBUNAM: CNIN: MA946	54.0	16.0	3.0	13.0	3.5	–	–	–	10.0
Spec. ID	AFW	ATL	FwL	HwL	MsFL	MsTL	MFL	MTL	AFW
CEUAEM-MAN-140	1.0	6.0	33.0	30.5	10.0	9.0	13.0	13.0	1.0
CEUAEM-MAN-135	1.0	6.0	32.0	31.0	10.0	9.0	13.0	13.0	1.0
CEUAEM-MAN-013	1.5	7.0	35.0	34.0	11.0	10.0	13.0	13.0	1.5
CEUAEM-MAN-021	1.0	5.0	31.0	27.0	10.0	9.0	11.0	12.0	1.0
CEUAEM-MAN-015	1.5	0.0	34.0	31.5	10.0	9.0	13.0	12.0	1.5
CEUAEM-MAN-014	1.5	6.0	34.0	31.0	10.5	9.5	13.0	13.0	1.5
IBUNAM: CNIN: MA645	–	6.0	–	–	–	–	15.0	14.5	–
IBUNAM: CNIN: MA810	–	5.0	–	–	–	–	14.0	15.0	–
IBUNAM: CNIN: MA946	–	4.5	–	–	–	–	–	–	–

subequal in length; distal cercomere smaller, conical, rounded at apex. Genitalia: left phallomere, sclerite L4B almost rectangular, longer than wide, with left margin projected anteriorly (Fig. 7a). Anterior lobe of phalloid apophysis (aafa) linguiform, sometimes oval, distally dentate. Posterior lobe of phalloid apophysis (pafa) elongated, apically rounded, dentate, bearing 3-6 ventral denticles. Posteromesal lobe (loa) oval, bearing short setae. Posterior process (paa) robust, sometimes slender. Right phallomere: triangular (Fig. 7b); posterior apex rounded with short setae. Dextral extension (bm) thick, slightly elongate; anterior extension of sclerite R3 (an) elongate, slender. Process anteromesal to pia (pva) short, thick, smooth with rounded apex; process posterolateral to pva (pia) short, smooth. Ventral phallomere: sclerite L4A oval (Fig. 7c, d). Secondary spine (ssp) well-sclerotized, triangular. Posterior process (pda) corkscrew-shaped, twisted left or right, with apex angled to slightly flattened.

Female (Fig. 8). Measurements (Table 3). Head: head capsule with oval eyes; juxtaocular bulges absent; ocellar tubercles absent; ocelli smaller than in males. Anterior margin of vertex straight; vertex slightly depressed near parietal sulcus. Antennae filiform; scape almost twice as long as pedicel. Frons wider than long in frontal view, with M-shaped depression in the middle of transverse carina (Fig. 9a). Thorax: pronotum, supracoxal dilation slightly pronounced; supracoxal groove well-marked. Lateral margins of prozone denticulate; lateral margins of metazone denticulate, becoming smooth distally; medial keel of pronotum well-developed. In ventral view, intercoxal area brownish. Legs: forelegs, spination formula: F = 4DS/14-16AvS/4PvS; T = 12-14AvS/8-10PvS. Forecoxae (Fig. 9b) armed with 3-6 apically blunt spines, often brownish, denticles interspersed among them; forecoxal lobes convergent. Forefemur relatively long, slender; femoral brush located at the level of last 3 posteroventral spines; tibial spur groove located at approximately half the length of femur; first discoidal spine smaller than the others; third discoidal spine longer than the others; with blackish spot at the level of first anteroventral spine (AvS). Foretarsus: distal portion of each segment blackish (Fig. 9c, d). Wings (fig. 10a-c): reaching approximately 3/4 the length of abdomen. Forewings: anterior margin wide at base, narrowing distally; color variable, ranging

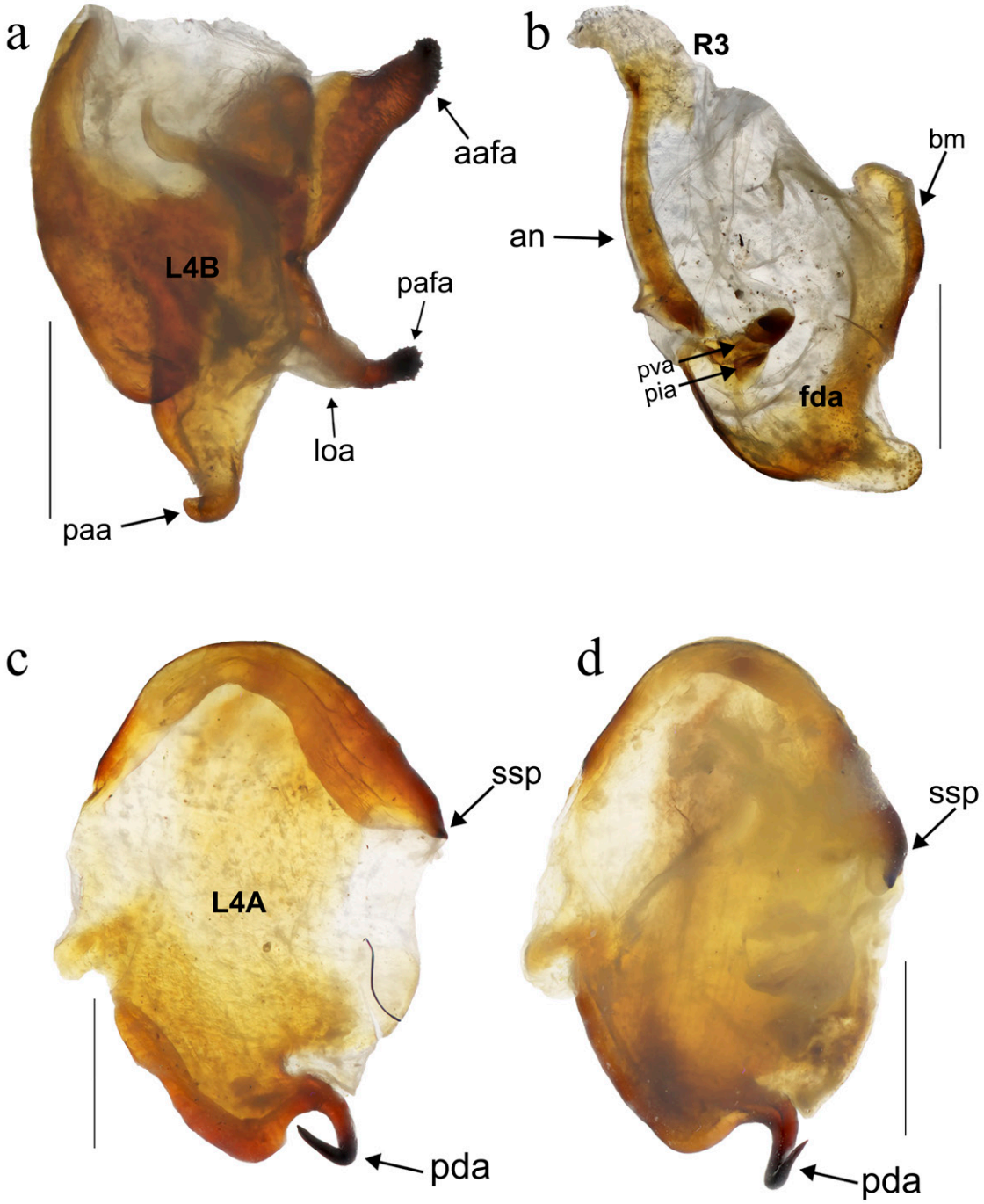

Figure 7. Male genitalia of *Stagmomantis hebardi*. a) Left phallomere in dorsal view; b) right phallomere in ventral view; c) ventral phallomere in dorsal view (sinistral morphotype); d) ventral phallomere in dorsal view (dextral morphotype). Specimen imaged: CEUAEM-MAN-021. Nomenclature follows Brannoch et al. (2017). See Table 1 for abbreviations. Scale bar = 1 mm.

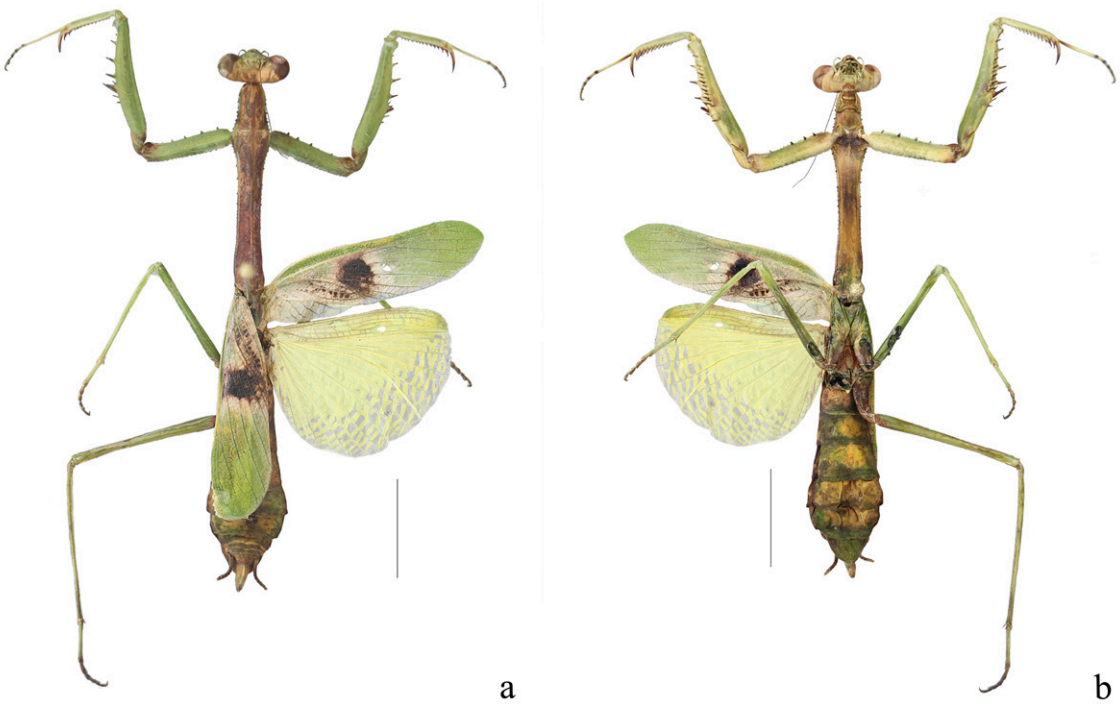

Figure 8. Female of *Stagmomantis hebardi* (green morphotype). a) Dorsal view; b) ventral view. Specimen imaged: CEUAEM-MAN-138. Scale bars = 10 mm.

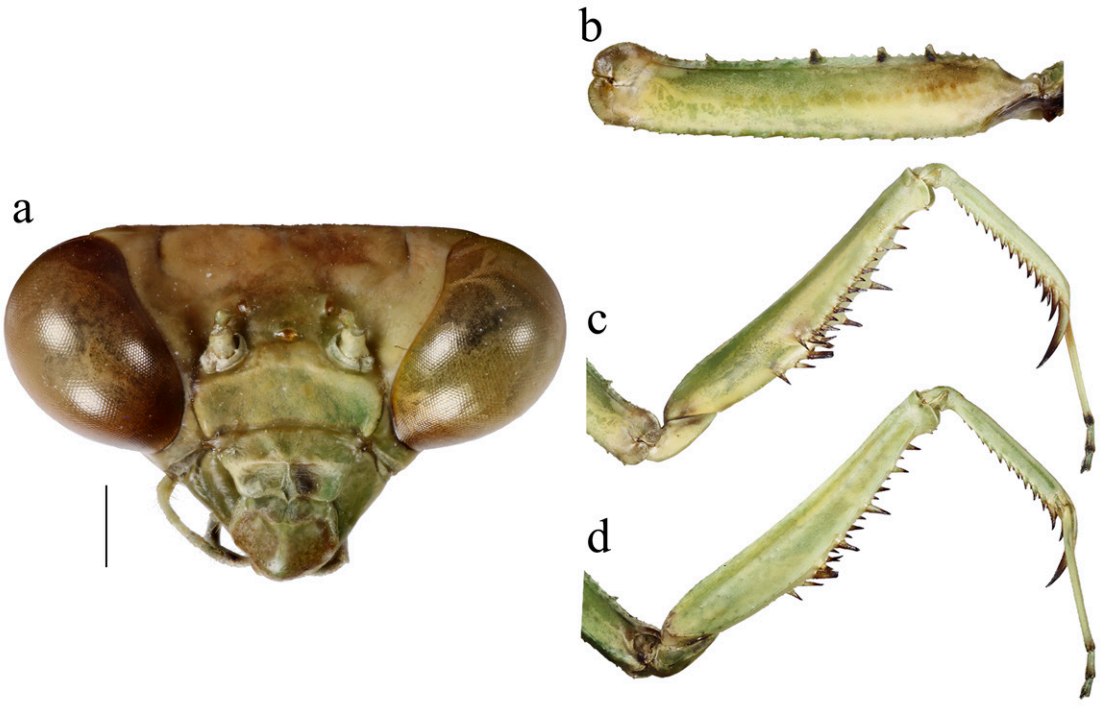

Figure 9. Morphological details of the female of *Stagmomantis hebardi*. a) Head capsule in frontal view; b) forecoxae in ventral view; c) forefemur and foretibia in ventral view; d) forefemur and foretibia in dorsal view. Specimen imaged: CEUAEM-MAN-138. Scale bar = 1 mm (a); not to scale (b-d).

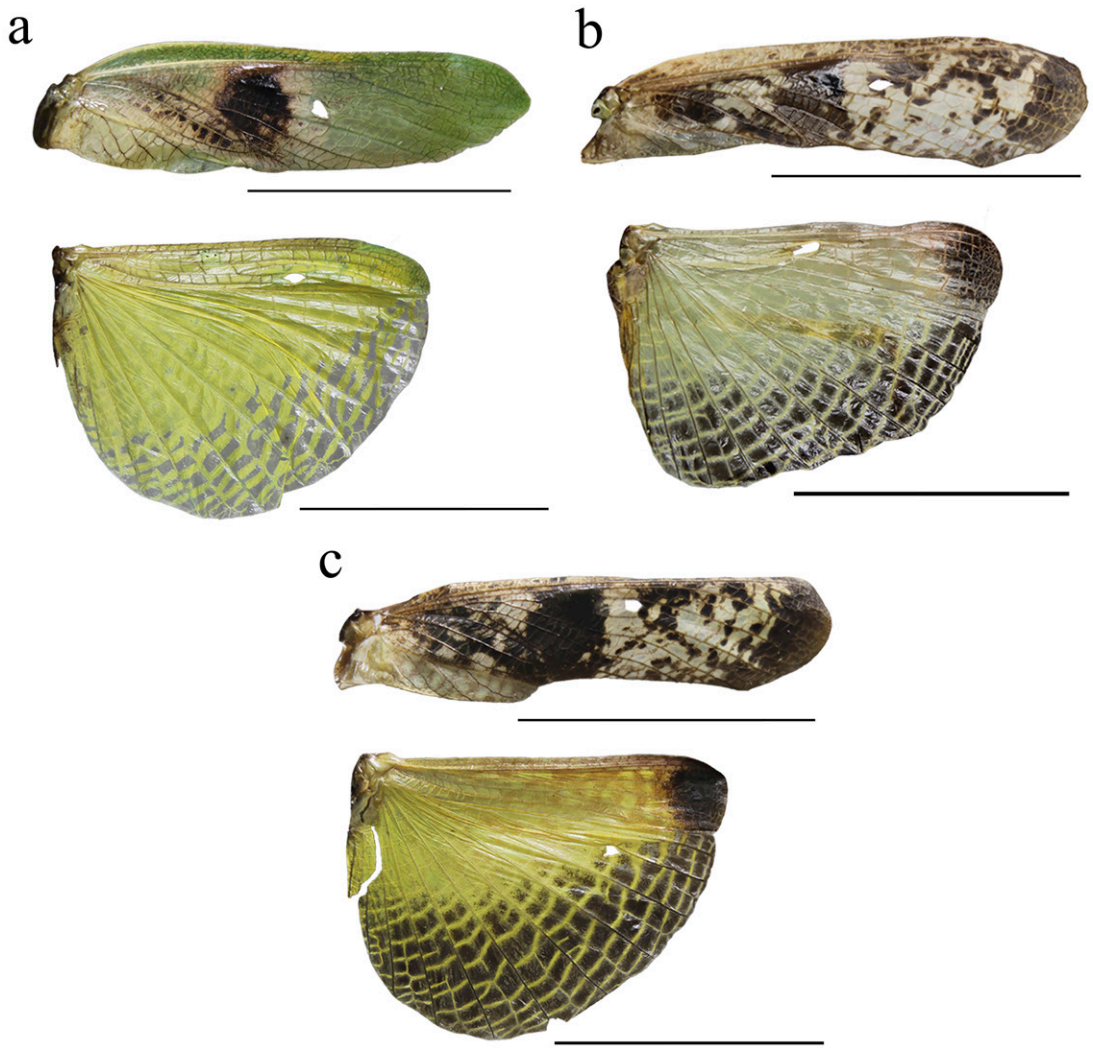

Figure 10. Fore- and hindwing variation in female *Stagmomantis hebardi*. a) Green morphotype; b) light brown morphotype; c) dark brown morphotype. Specimens imaged: a (CEUAEM-MAN-138); b (CEUAEM-MAN-129); c (CEUAEM-MAN-139). Scale bars = 10 mm.

from brown to light hues; stigma darker than rest of wing. Hindwings fully colored; color variable, ranging from yellowish at base to middle area, with dark spots distally, to yellowish with hyaline spot; apex of hindwing yellowish with greenish portions. Abdomen: dorsoventrally flattened, reaching maximum width between 4th and 6th tergites, with prominent, protrusible lobe-like structure between 5th and 6th tergites. Supragenital plate wider than long, rounded at the apex, with a marked longitudinal medial keel. Cerci elongate; cercomeres cylindrical, subequal in length; distal cercomere smaller, conical, apically rounded.

Genitalia (Fig. 11): gonoplacs (gl9), simple, elongate, apically rounded, bearing short setae throughout, with longer setae apically. Gonapophysis: gonapophysis 9 (gp9) membranous, elongate, shorter than gl9. Gonapophysis 8 (gp8) elongate, bearing short setae; in lateral view, distinct furrow near ventral margin; lateral margins sinuous depressed near base of apical lobe (gpal8). Apical lobe of gonapophysis 8 (gpal8) glove-shaped; dorsal portion laterally compressed, distally rounded; ventral portion short, elongate; surface covered with short setae, longer setae on inner surface. Medial outgrowth of gonapophysis 8 (gpmo8) well-developed. Coxa 8 (CX8): acuminate,

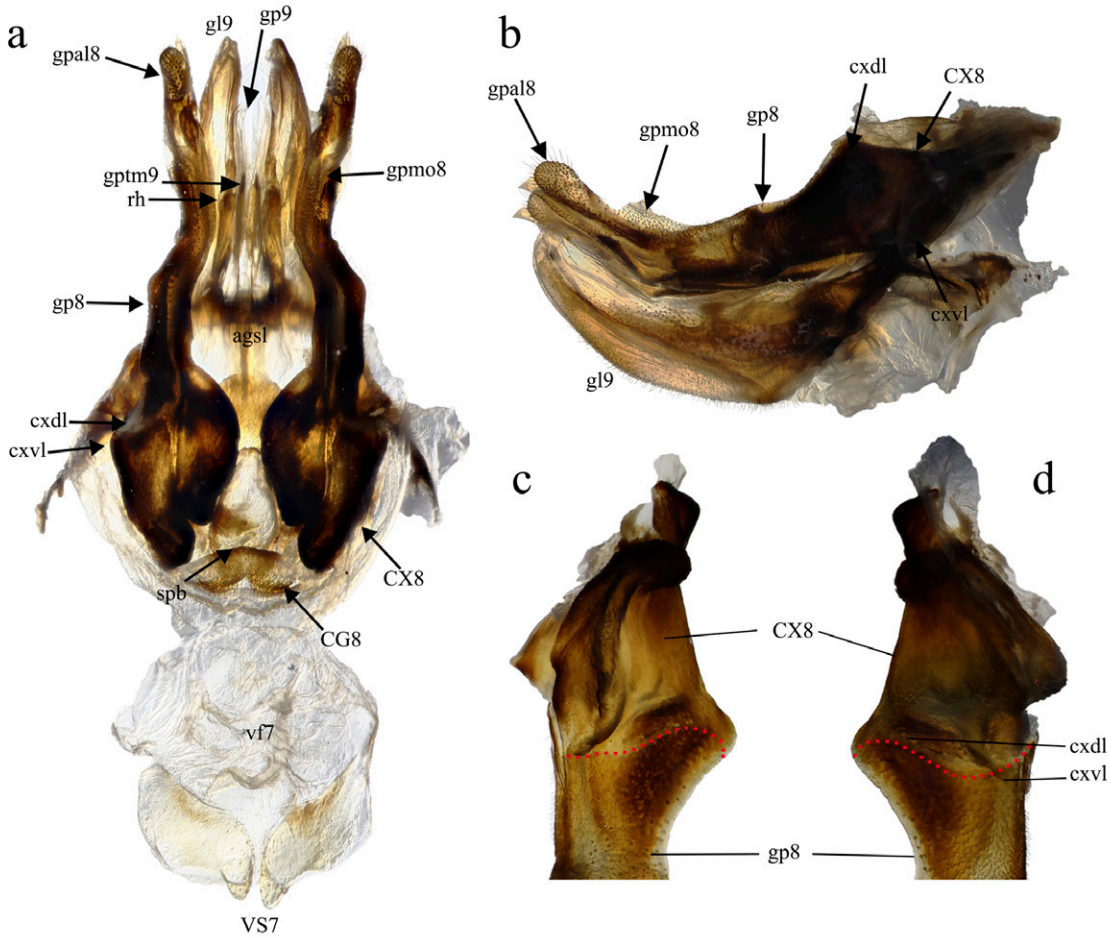

Figure 11. Female genitalia of *Stagmomantis hebardi*. a) Ventral view of the ovipositor (upper half) and ventral fold (lower half); b) ovipositor in lateral view; c-d) close-up of coxa 8 (cx8) and the distal third of gonapophysis 8 (gp8): c) ventral aspect in lateral view; d) dorsal aspect in lateral view. The red line indicates the boundary between CX8 and gp8. Specimens imaged: a (CEUAEM-MAN-162); b (CEUAEM-MAN-161); c-d (CEUAEM-MAN-160). Nomenclature follows Brannoch et al. (2017). See Table 1 for abbreviations.

broad, rounded at base, tapering distally; divided into dorsal and ventral regions by a marked depression, a prominent keel extending through middle of depression. Dorsal region of CX8 elongate lateral wider, more rounded than dorsal region. Caudogyne (CG8) weakly sclerotized; dorsal margin rounded, sinuous; ventral margin depressed at the middle (M-shaped). Spermathecal bulge (spb) well-sclerotized. Accessory gland supporting lobe (agsl) smooth, weakly sclerotized. Ventral segmental fold 7 (vf7) membranous, rounded, with sinuous margins. Vestibular sclerite (VS7) weakly sclerotized, rhomboidal in shape, with ventro-medial corner rounded.

Taxonomic summary

Holotype: 1 ♀, Mexico. Sinaloa: Venvidio, 2-6. VIII.1918, type # 8988 (ANSP). Allotype: 1 ♀, Sinaloa: Los Mochis, 25.XII.1918 (ANSP). Additional material examined: Mexico. Estado de México: 1 ♂, Nepantla, Finca Badoni, 18°59’0.8” N, 98°50’44.9” W, 2,020 m asl, 05.X.2023 (CEUAEM-MAN-135); 1 ♀, Malinalco, Chalma, 118°55’56.3” N, 99°26’11” W, 29.XI.1980 (IBUNAM: CNIN: MA909). Guerrero: 10 specimens (5 ♂, 5 ♀). Five ♂: Acahuizotla, 17°28’8.9” N, 99°25’10.3” W, 18.XI.1983 (IBUNAM: CNIN: MA644, MA645); Iguala, Km 3 desv. a Tepecoacuilco, 18°17’32” N, 99°28’58” W,

Table 3
Measurements (in mm) of females of *Stagmomantis hebardi* (*n* = 9).

Spec. ID	TL	PL	PrL	ML	PW	HH	HW	ACL	AFL
CEUAEM-MAN-139	52.0	20.0	4.5	15.5	4.0	4.5	7.0	10.0	13.0
CEUAEM-MAN-129	48.0	18.0	3.5	15.0	3.0	4.2	6.0	9.0	11.5
CEUAEM-MAN-019	48.0	20.0	4.5	15.5	3.8	4.5	7.0	9.5	12.0
CEUAEM-MAN-018	49.0	21.0	4.5	17.0	4.0	4.5	6.5	10.0	13.0
CEUAEM-MAN-017	51.0	20.0	4.5	15.5	4.0	5.0	7.0	10.0	13.0
CEUAEM-MAN-138	53.0	20.0	4.5	16.0	4.0	5.0	7.0	10.5	13.0
CEUAEM-MAN-109	48.0	19.5	4.0	15.5	4.0	4.0	7.0	9.5	12.5
IBUNAM: CNIN: MA1560	55.0	23.0	5.0	18.0	4.0	–	–	–	13.0
IBUNAM: CNIN: MA946	54.0	16.0	3.0	13.0	3.5	–	–	–	10.0
Spec. ID	AFW	ATL	FWL	HWL	MsTL	MFL	MFL	MTL	AFW
CEUAEM-MAN-139	1.5	8.0	19.5	17.0	12.0	10.5	14.5	15.5	1.5
CEUAEM-MAN-129	1.5	7.0	19.0	17.0	11.0	10.0	14.0	15.0	1.5
CEUAEM-MAN-019	2.0	8.0	–	–	12	11	15.0	16.0	2.0
CEUAEM-MAN-018	2.0	8.0	21.0	–	12	11	15.0	15.5	2.0
CEUAEM-MAN-017	2.0	8.0	–	17.0	12.0	11.0	16.0	16.0	2.0
CEUAEM-MAN-138	2.0	8.0	22.0	18.0	12.0	11.5	16.0	16.0	2.0
CEUAEM-MAN-109	2.0	6.5	20.0	16.0	12.0	11.0	15.0	15.0	2.0
IBUNAM: CNIN: MA1560	–	6.5	–	–	–	–	17.0	16.0	–
IBUNAM: CNIN: MA946	–	7.0	–	–	–	–	17.5	18.0	–

14.X.2006 (IBUNAM: CNIN: MA724); Iguala, Tuxpan, 2 km a Microondas, 18°23’34” N, 99°28’27” W, 14.X.2006 (IBUNAM: CNIN: MA813); Tecpan, La Laguna, Km 15 San Luis, 17°13’14.9” N, 100°37’9.3” W, 1,425 m asl, 20.VII.2005 (IBUNAM: CNIN: MA816). Five ♀: Atenango del Río, Km 36 Huitzuco-Atenango, 18°8’32” N, 99°7’49” W, 200 m asl, 14.X.2006 (IBUNAM: CNIN: MA823); Guerrero, 22.IX.2022 (CEUAEM-MAN-159, CEUAEM-MAN-160); Guerrero, 2024 (CEUAEM-MAN-161, CEUAEM-MAN-162). Jalisco: 13 specimens (11 ♂, 2 ♀). Eleven ♂: La Huerta, Estación de Biología Chamela (UNAM), 19°29’55.2” N, 105°2’39.5” W, 01.VIII.1981 (IBUNAM: CNIN: MA426); 10.V.1980 (IBUNAM: CNIN: MA802, MA804); 24.V.1980 (IBUNAM: CNIN: MA803); 10.VIII.1981 (IBUNAM: CNIN: MA805-MA810); 01.IV.1981 (IBUNAM: CNIN: MA811). Two ♀: La Huerta, Estación de Biología Chamela (UNAM), 19°29’55.2” N, 105°2’39.5” W, 14.X.1990 (IBUNAM: CNIN: MA723); 08.VIII.1975 (IBUNAM: CNIN: MA1560). Morelos: 23 specimens (12 ♂, 11 ♀). 12 ♂: Jojutla, EESJ, 18°36’49.8” N, 99°13’50.2” W, 957 m asl: 08.III.2022 (CEUAEM-MAN-013); 07.X.2018 (CEUAEM-MAN-014); 21.XI.2018 (CEUAEM-MAN-015); 20.XI.2019 (CEUAEM-MAN-021); Jojutla, 18°36’41.6” N, 99°10’44.7” W, 894 m asl, 21.X.2023 (CEUAEM-MAN-140); Morelos, 18°39’3.9” N, 99°2’20.5” W, 16.XI.1972 (IBUNAM: CNIN: MA519, MA520); Tepalcingo, Sierra de Huautla, 18°32’31.3” N, 98°56’9.4” W, 12.VI.2016 (IBUNAM: CNIN: MA943-MA946). Eleven ♀: Zacatepec, Galeana, 18°38’24.1” N, 99°12’39.6” W, 934 m asl, 22.IX.2019 (CEUAEM-MAN-017); Jojutla, EESJ, 18°36’49.8” N, 99°13’50.2” W, 957 m asl: 28.XI.2019 (CEUAEM-MAN-018); 22.XI.2019 (CEUAEM-MAN-019); 25.IX.2020 (CEUAEM-MAN-109); 13.XI.2020 (CEUAEM-MAN-110); 04.X.2023 (CEUAEM-MAN-129); Tehuixtla, 18°33’16.8” N, 99°16’12.8” W, 26.XII.2019 (CEUAEM-MAN-072); Yautepec, 18°53’12.8” N, 99°3’47.8” W, 1,216 m asl, 17.X.2023 (CEUAEM-MAN-138); Jojutla, 18°36’41.6” N, 99°10’44.7” W, 894 m asl, 27.X.2023 (CEUAEM-MAN-139); Cuautla, 18°48’59.4” N, 98°56’56” W, XI.1954 (IBUNAM: CNIN: MA905); Morelos, 18°39’3.9’’ N, 99°2’20.5” W, IV.1981 (IBUNAM: CNIN: MA906). Nayarit: 1 ♂, Bahía de Banderas, San Rafael, Arroyo de

la Virgen, P. H. Aguamilpa, 20°50'19.5" N,105°16'44.4" W, 734 m asl, 01.XI.1991 (IBUNAM: CNIN: MA824).

Geographic distribution: *Stagmomantis hebardi* is distributed in the states of Estado de México, Guerrero, Jalisco, Morelos, Nayarit, and Sinaloa (Fig. 12).

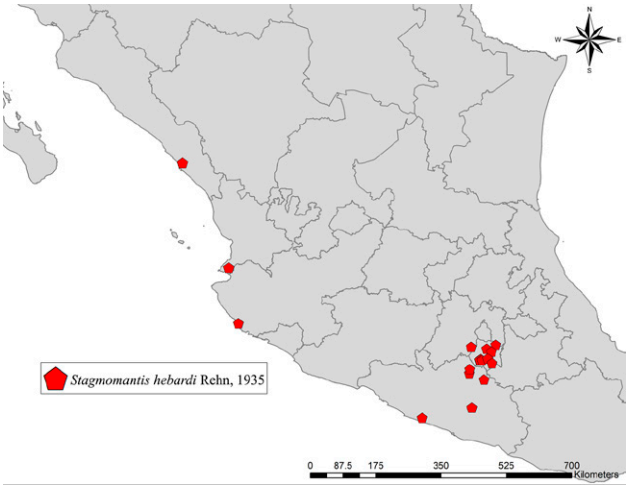

Figure 12. Geographic distribution of examined specimens of *Stagmomantis hebardi* in Mexico.

Remarks

Taxonomic delimitation within *Stagmomantis* based on male morphology has been a subject of study for decades. Notably, Saussure and Zehntner (1894) and Rehn (1935) considered the males of *S. carolina* and *S. tolteca* to be indistinguishable, grouping them within the "carolina group," which currently corresponds to the subgenus *Stagmomantis*.

Morphological differences between the female originally described by Rehn (1935) and the females analyzed in this study are summarized in Table 4. Key distinctions include: *a)* the pronotum is proportionately wider in Rehn's female compared to the slender pronotum in our specimens; *b)* wing shape and coloration differ significantly; Rehn's specimen has wider forewings with a small, oval, light-colored stigma lacking a surrounding patch, whereas our specimens exhibit a stigma covered by a dark patch and surrounded by a white area covering nearly the proximal half of the wing; *c)* the abdomen in Rehn's female is widely oval, whereas it is subfusiform (widening at the distal segments) in the females observed in this study; and *d)* the lobe-like structure between the 5th and 6th abdominal tergites, observed in all examined specimens, appears to be a diagnostic feature and a potential autapomorphy for this species.

Although *Stagmomantis tolteca* and *S. hebardi* are morphologically similar, significant differences in male genitalia provide reliable diagnostic characters. As noted by Arteaga-Blanco et al. (2016), the posterior process of the ventral phallomere (pda) in *S. tolteca* is strongly sclerotized, wide at the base, tapering distally into a spine, and directed sinistrally (Fig. 13a, blue). Conversely, in *S. hebardi*, the pda is corkscrew-shaped, twisted either sinistrally or dextrally (Figs. 1, 5, 13b, blue). Further comparisons revealed differences in other genitalic structures: the aafa in *S. tolteca* is triangular with an angulate apex (Fig. 13a, yellow), whereas it is rounded in *S. hebardi* (Figs. 5, 13b, yellow); the ssp in *S. tolteca* is more developed with a slightly angulate inferior margin (Fig. 13a, purple), compared to the small and triangular ssp in *S. hebardi* (Figs. 5, 13b, purple); finally, the pafa in *S. tolteca* is elongate and curved near the middle, with the apex directed inward (Fig. 13a, green), while the pafa of *S. hebardi* projects laterally, is less curved, and has a more rounded apex (Figs. 5, 13b, green). The paa is morphologically similar in both species (Fig. 13, red). Rehn's (1935) illustrations of the male genitalia correspond more closely to the pda morphology described in the present study than to

Table 4

Comparison between the female of *Stagmomantis hebardi* in Rehn (1935) and the female specimens examined in this study.

Rehn (1935)	Present study
Pronotum wide	Pronotum slender
Forewings solid light colored	Forewings with different combinations of colors
Forewing's stigma not covered by a colored patch	Forewing's stigma covered by a white and dark patch
Forewings wider	Forewings slender
Abdomen wider almost oval	Abdomen subfusiform
Abdomen without lobe-like structure	Abdomen with lobe-like structure

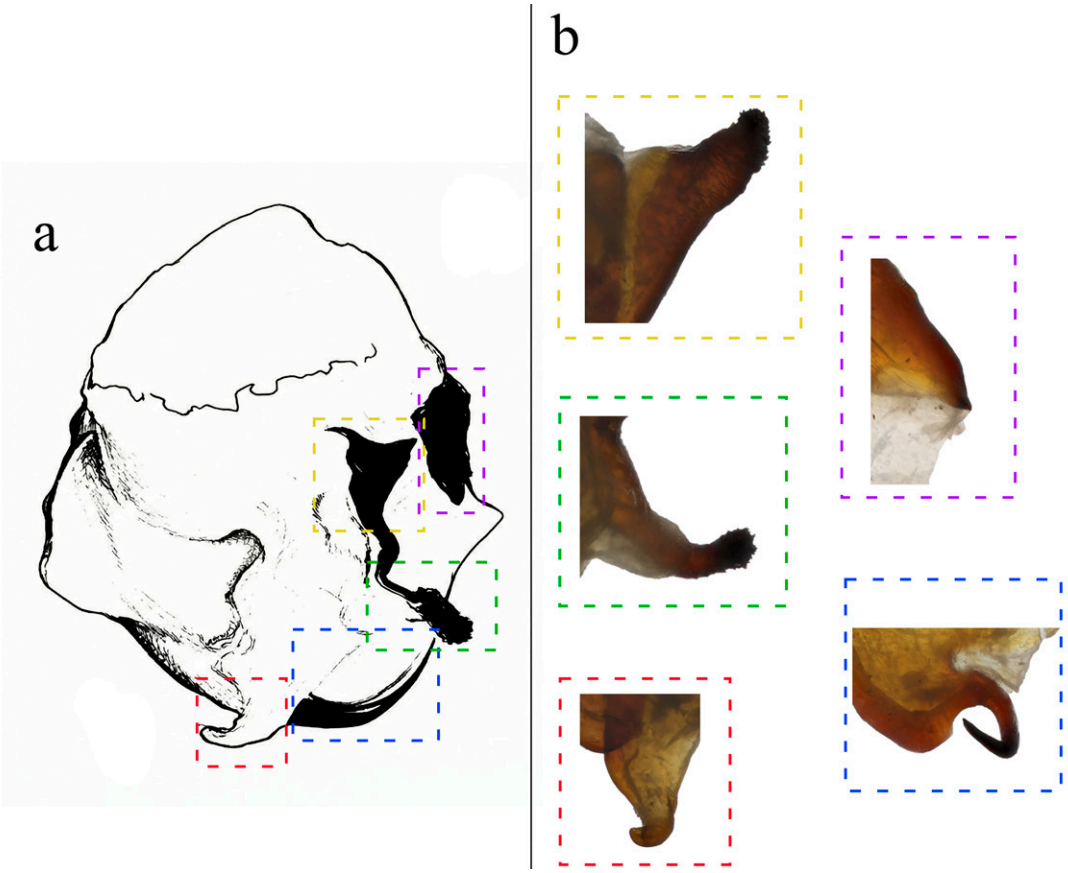

Figure 13. Comparison of male genitalia. a) *Stagmomantis tolteca*, modified from Arteaga-Blanco et al. (2016); b) *Stagmomantis hebardi*. Color coding: blue = pda; green = pafa; purple = ssp; red = paa; yellow = aafa. Specimen imaged: CEUAEM-MAN-021. See Table 1 for abbreviations.

that illustrated in Arteaga-Blanco et al. (2016). Thus, the sclerotized structure of the pda serves as a robust diagnostic character to separate both species and supports the identification of our male specimens as *S. hebardi*, in accordance with Rehn (1935).

A remarkable feature observed in this study is the presence of a lobe-like structure on the female abdomen. While comparable structures are rare in Mantodea, a few instances have been documented. For example, Robinson and Robinson (1979) described a terminal abdominal structure in females of *Acanthops falcata* Stål, 1877, identifying it as a pheromone-releasing gland. Similarly, Schwarz and Glaw (2021) described a Y-shaped protrusible structure near the abdominal apex of *Stenophylla lobivertex* Lombardo, 2000, hypothesizing that it represents a pheromone-releasing gland more efficient than simpler structures performing the same function.

The precise function of the lobe-like structure identified in this study remains unknown; however, several hypotheses can be proposed. According to Robinson and Robinson (1979) and Schwarz and Glaw (2021), such structures may function as sex pheromone glands, as reported for *A. falcata* and *S. lobivertex*. However, we observed this structure in both sexes during the early developmental stages of *S. hebardi*, which suggests it may possess an alternative or additional function. Another hypothesis involves the release of prey-attracting pheromones (kairomones), similar to the aggressive mimicry observed in bolas spiders (*Mastophora* Holmberg, 1876), which mimic lepidopteran sex pheromones to capture prey (Yeargan & Quate, 1997). Finally, this structure might enhance crypsis, similar to strategies observed in the subfamily Vatinae. However, unlike Vatinae, which are characterized by fixed cuticular lobes on the legs or abdominal margins, the structure in *S. hebardi* is distinctively protrusible.

Acknowledgements

We thank Cristina Mayorga-Martínez for her support in reviewing the CNIN-IBUNAM; Michael R. Maxwell, Henrique M. Rodrigues, and Lohitashwa Garikipati for their comments on an earlier version of this work; Jason D. Weintraub for providing us high resolution images of the holotype and allotype of *Stagmomantis hebardi*. Aarón Emilio Vásquez Quintero was supported by a scholarship from the Secretaría de Ciencia, Humanidades, Tecnología e Innovación (Secihti; CVU 1315459).

References

Agudelo-Rondón, A. A., & Chica, E. L. M. (2002). *Mántidos. Introducción al conocimiento del orden Mantodea*. Universidad Distrital Francisco José de Caldas, Bogotá, Colombia.

Agudelo-Rondón, A. A., Lombardo, F., & Jantsch, L. J. (2007). Checklist of the Neotropical mantids (Insecta, Dictyoptera, Mantodea). *Biota Colombiana*, *8*, 105–158.

Anderson, K. (2020a). Revision of *Stagmomantis* Saussure, 1869. *Soothsayer, Journal of Mantodea Research*, *1*, 9–18.

Anderson, K. (2020b). Revalidation of *Stagmomantis* (Stagmomantis) *conspurcata* (Serville, 1839). *Soothsayer, Journal of Mantodea Research*, *1*, 1–20.

Anderson, K. (2021). A new species of *Stagmomantis* Saussure, 1869 from North America. *Soothsayer, Journal of Mantodea Research*, *2*, 86–96.

Anderson, K. (2025). *Mantodea mundi: comprehensive nomenclatural catalogue of Mantodea (September 2025 edition)*. On line resource available at: file:///C:/Users/joelv/Downloads/MantodeaMundi09.25.pdf

Arteaga-Blanco, L. A., de la Parra-Guerra, A. C., & Martínez-Hernández, N. J. (2016). Descripciones taxonómicas de mántidos (Insecta: Mantodea) del Departamento del Atlántico, Colombia, con apuntes sobre su distribución. *Boletín Científico Centro de Museos. Museo de Historia Natural*, *20*, 211–236. https://doi.org/10.17151/bccm.2016.20.1.16

Brannoch, S. K., Wieland, F., Rivera, J., Klass, K. D., Olivier, B., & Svenson G. J. (2017). Manual of praying mantis morphology, nomenclature, and practices (Insecta, Mantodea). *Zookeys*, *696*, 1–100. https://doi.org/10.3897/zookeys.696.12542

Ehrmann, R. (2002). *Mantodea: Gottesanbeterinnen der Welt*. Natur und Tier-Verlag. Münster, German.

Ferraz, B. R., Souza-Dias, P. G. B., & Rivera, J. (2023). A hidden gem from northeastern Brazil: a new species of *Metaphotina* Piza, 1964 (Mantodea, Acontistidae) ecologically linked to the Caatinga. *Zootaxa*, *5343*, 31–54. https://doi.org/10.11646/zootaxa.5343.1.2

Garikipati, L. (2024). Description and total ontogeny of the Sonoran tiger mantis, *Stagmomantis clauseni* sp. nov., and key to the subgenus *Nigralora* (Mantodea: Mantidae). *Zootaxa*, *5501*, 079–107. https://doi.org/10.11646/zootaxa.5501.1.4

Hebard, M. (1923). Dermaptera and Orthoptera from the state of Sinaloa, Mexico. *Transactions of the American Entomological Society (1890-)*, *48*, 157–196.

INEGI (Instituto Nacional de Estadística y Geografía). (2024). Área geoestadística estatal, escala: 1:250000. Instituto Nacional de Estadística y Geografía. México, Ciudad de México. Retrieved March 23, 2025 from: https://www.inegi.org.mx/app/biblioteca/ficha.html?upc=794551132173

Maxwell, M. R. (2014). A synoptic review of the genus *Stagmomantis* (Mantodea: Mantidae). *Zootaxa*, *3765*, 501–525. https://doi.org/10.11646/zootaxa.3765.6.1

Otte, D., & Spearman, L. (2005). *Mantida species file. Catalog of the mantids of the world*. Philadelphia: Association of Insect Diversity.

Patel, S., & Singh, R. (2016). Updated checklist and distribution of Mantidae (Mantodea: Insecta) of the world. *International Journal of Research Studies in Zoology*, *2*, 17–54. https://doi.org/10.20431/2454-941X.0204003

Rehn, J. A. G. (1935). On certain Mexican and Central American species of *Melliera* and *Stagmomantis* (Orthoptera, Mantidae). *Transactions of the American Entomological Society*, *61*, 317–329.

Robinson, H. M., & Robinson, B. (1979). By dawn's early light: matutinal mating and sex attractants in a Neotropical mantid. *Science*, *205*, 825–827. https://doi.org/10.1126/science.205.4408.825

Rodrigues, H. M., & Cancello, E. M. (2016). Taxonomic revision of *Stagmatoptera* Burmeister, 1838 (Mantodea: Mantidae, Stagmatopterinae). *Zootaxa*, *4183*, 1–78. https://doi.org/10.11646/zootaxa.4183.1.1

Saussure, H., & Zehntner, L. (1894). Fam. Mantidae. In H. Saussure, & L. Zehntner, A. (Eds.), *Biologia Centrali-Americana, Insecta. Orthoptera, Vol. 1* (pp. 123–197). Paris: L'Imprimerie Nationale.

Schwarz, C. J., & Glaw, F. (2021). The luring mantid: protrusible pheromone glands in *Stenophylla lobivertex* (Mantodea: Acanthopidae). *Journal of Orthoptera Research*, *30*, 31–33. https://doi.org/10.3897/jor.30.55274

Schwarz, C. J., & Roy, R. (2019). The systematics of Mantodea revisited: an updated classification incorporating multiple data sources (Insecta: Dictyoptera). *Annales de La Société Entomologique de France*, *55*, 101–196. https://doi.org/10.1080/00379271.2018.1556567

Su, Y. N. (2016). A simple and quick method of displaying liquid-preserved morphological structures for microphotography. *Zootaxa*, *4208*, 592–593. https://doi.org/10.11646/zootaxa.4208.6.6

Svenson, G. J., & Whiting, M. F. (2004). Phylogeny of Mantodea based on molecular data: evolution of a charismatic predator. *Systematic Entomology*, *29*, 359–370.

Svenson, G. J., & Whiting, M. F. (2009). Reconstructing the origins of praying mantises (Dictyoptera, Mantodea): the roles of Gondwanan vicariance and morphological

convergence. *Cladistics*, *25*, 468–514. https://doi.org/10.1111/j.1096-0031.2009.00263.x

Terra, P. S. (1995). Revisão sistemática dos gêneros de louva-a-deus da região Neotropical (Mantodea). *Revista Brasileira de Entomologia*, *39*, 13−94.

Varela-Hernández, F., Martínez-Luque, E. O., Vázquez-Franco, C. M., & Pedraza-Lara, C. (2022). Contribution to the knowledge of mantids (Insecta, Mantodea) in Central Mexico: a morphological and molecular approach. *Southwestern Entomologist*, *47*, 27–43.

Wang, W., Wang, H., Huang, H., Zhao, Y., & Zhou, Z. (2022). Mitochondrial genomes of 10 Mantidae species and their phylogenetic implications. *Archives of Insect Biochemistry and Physiology*, *111*, e21874. https://doi.org/10.1002/arch.21874

Xu, X. D., Guan, J. Y., Zhang, Z. Y., Cao, Y. R., Storey, K. B., Yu, D. N. et al. (2021). Novel tRNA gene rearrangements in the mitochondrial genomes of praying mantises (Mantodea: Mantidae): translocation, duplication and pseudogenization. *International Journal of Biological Macromolecules*, *185*, 403–411. https://doi.org/10.1016/j.ijbiomac.2021.06.096

Yeargan, K. V., & Quate, L. W. (1997). Adult male bolas spiders retain juvenile hunting tactics. *Oecologia*, *112*, 572–576. https://doi.org/10.1007/s004420050347